Korean J. Chem. Eng., **31**(4), 701-705 (2014)
DOI: 10.1007/s11814-013-0275-5

pISSN: 0256-1115
eISSN: 1975-7220

CO_2 absorption characteristics of a jet loop reactor with a two-fluid swirl nozzle in an alkaline solution

Go-Eun Cha*, Ho-Jin Sung, Jun-Heok Lim***, Tae-Yoon Lee*, and Jea-Keun Lee*,†**

*Department of Environmental Engineering, Pukyong National University, Busan 608-737, Korea
**Institute for Advanced Engineering, Gyeonggy 449-863, Korea
***Department of Chemical Engineering, Pukyong National University, Busan 608-739, Korea
(*Received 7 August 2013 • accepted 13 December 2013*)

Abstract−To investigate the performance of a jet loop reactor with the two-fluid swirl nozzle (TSN), CO_2 absorption experiments in an alkaline solution were performed. The experimental results obtained in the reactor were compared with those in a jet loop reactor with the two-fluid conventional nozzle (TCN). The neutralization time of alkaline solution and the CO_2 removal efficiency were used as the indices for a comparison of the reactor performance. Due to the swirling flow, the neutralization times of alkaline solutions by CO_2 in the reactor with the TSN were shortened compared with those in the reactor with the TCN. Also, the instantaneous and/or overall CO_2 removal efficiencies in the reactor with the TSN were higher than those in the reactor with the TCN at the same liquid circulation flow rate.

Keywords: Jet Loop Reactor, Two-fluid Swirl Nozzle, CO_2 Absorption, Neutralization Time, CO_2 Removal Efficiency

INTRODUCTION

The gas absorption efficiency of an absorption tower is largely affected by the gas residence time and the absorption rate [1]. Previous research topics focused around developing absorption equipment to improve gas absorption efficiency in gas-liquid systems. Accordingly, developments were made on many types of absorption equipment such as the packed tower [2], spray tower [3], bubble column [4,5], and agitated vessel [6], and such equipment was used in various fields.

Gaddis [7] reported that bubble columns are structurally simple and thus are easy to manufacture with corrosion-resistant materials, but show poor mass transfer performance compared to other equipment. The agitated vessel is characterized by its enhanced mass transfer rate due to the strong turbulence intensity in the liquid, which is created with the impeller and the small gas bubbles with a high surface area per unit volume, but it requires additional power to operate the impeller. Moreover, the packed tower has advantages of having a wide gas-liquid contact area because the system fills a packing material in the equipment and sprays liquid on it, but it has a disadvantage of high pressure drop.

Bohner et al. [8] developed a jet loop reactor that can form very small bubbles to achieve a higher absorption rate and to improve the turbulence intensity of the gas-liquid absorption system. The jet loop reactor forms very small bubbles due to the shear field induced by the liquid jet at the nozzle outlet when gases and liquids are sprayed from the two-fluid nozzle installed in the draft tube, which produces in a wide contact area between gas and liquid and a high turbulence intensity. Moreover, due to the small size of bubbles, the bubble residence time increases as the liquid flows down the draft tube and flows up through the annular space, and as parts of the gas and liquid recirculate in the upflow stream into the draft tube [9]. Such characteristics improve the mass transfer rate in the gas-liquid system. Therefore, studies are focused on advancing the application of such advantages to chemical and biological treatments, including gas-liquid systems, such as denitrification by ammonia stripping [10], removal of organic matter from piggery wastewater [11], aerobic treatment of winery wastewater [12], and neutralization of highly alkaline wastewater using CO_2 [13]. Recently, Lee and Son [14] devised a jet loop reactor with a two-fluid swirl nozzle (TSN) that forms swirling flow both inside and outside the draft tube when gas and liquid are sprayed through the nozzle tip. The jet loop reactor with the TSN produces smaller bubbles than those produced by the jet loop reactor with the two-fluid conventional nozzle (TCN), increases the turbulence intensity when gas and liquid pass the draft tube and the annular space, and is likely to further improve the mass transfer rate in the gas-liquid system.

We investigated the performance of a jet loop reactor with the TSN during CO_2 absorption in an alkaline solution and compared it with that of a jet loop reactor with a TCN. Their performance levels were compared based on the alkaline solution neutralization time and the CO_2 removal efficiency.

EXPERIMENT

The lab-scale jet loop reactor system that was used in this study (Fig. 1) consisted mainly of a jet loop reactor, a storage tank, a volumetric pump, a circulation pump, and a CO_2 bomb. The jet loop reactor used in this experiment had a downstream circular cylinder shape, and its interior consisted of a reaction tube, a draft tube, a gas-liquid separation tank, and a two-fluid nozzle. The reaction tube, draft tube, and gas-liquid separation tank were used with a transparent acryl that was shaped like a cylinder. The total height and effective volume of the jet loop reactor were 1 m and 28.5 L, re-

†To whom correspondence should be addressed.
E-mail: leejk@pknu.ac.kr

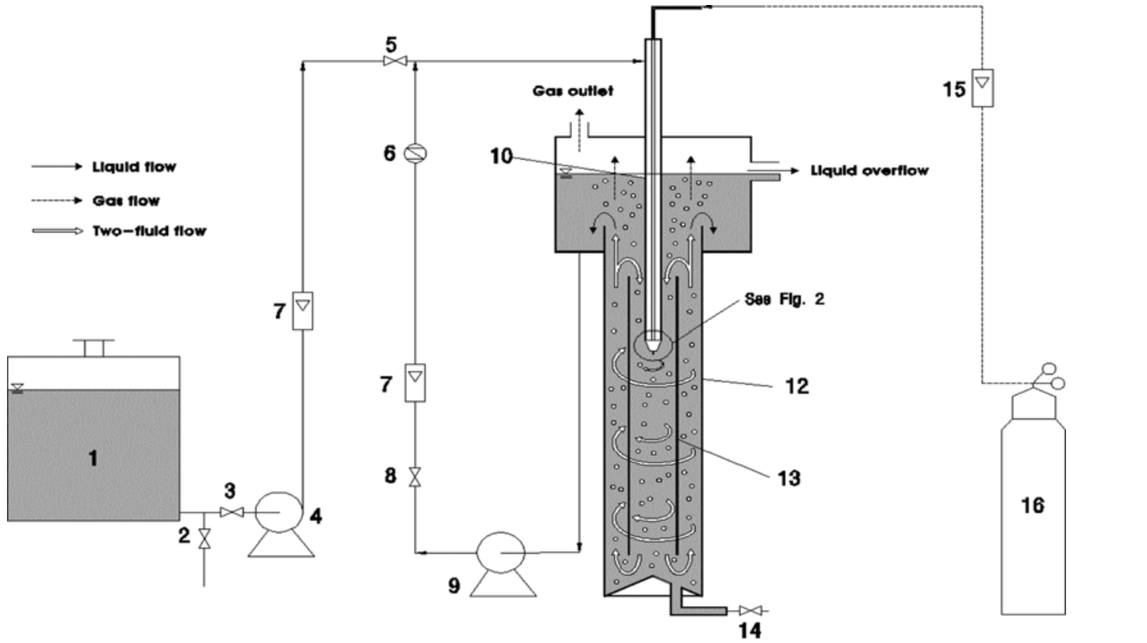

Fig. 1. Schematic of the experiment apparatus that was used in this study.

1. Storage tank
2. Sampling valve
3. Valve
4. Liquid induction volumetric valve
5. Valve
6. Check valve
7. Liquid flow meter
8. Valve
9. Circulation pump
10. Nozzle
11. Gas discharge valve
12. Jet loop reactor with two-fluid swirl nozzle (TSN)
13. Draft tube
14. Treatment solution discharge valve
15. Gas flow meter
16. CO_2 bomb

spectively. The height and the inner diameter of the reaction tube were 0.75 m and 0.10 m; of the draft tube, 0.60 m and 0.049 m; and of the gas-liquid separation tank, 0.35 m and 0.30 m, respectively.

The liquid induction tube of the two-fluid nozzle was used with a PVC tube with an inner diameter of 16 mm. The interior of the lower part of the nozzle was corn-shaped, and the inner diameter of the nozzle at the point that was 40 mm above the liquid nozzle tip gradually decreased to 5 mm at the liquid nozzle tip. The gas induction tube was used a stainless tube with an outer diameter of 3 mm, and was fixed coaxially at the center of the liquid induction tube. In this experiment, two types of nozzle as two-fluid nozzle (TCN and TSN) were used as shown in Fig. 2.

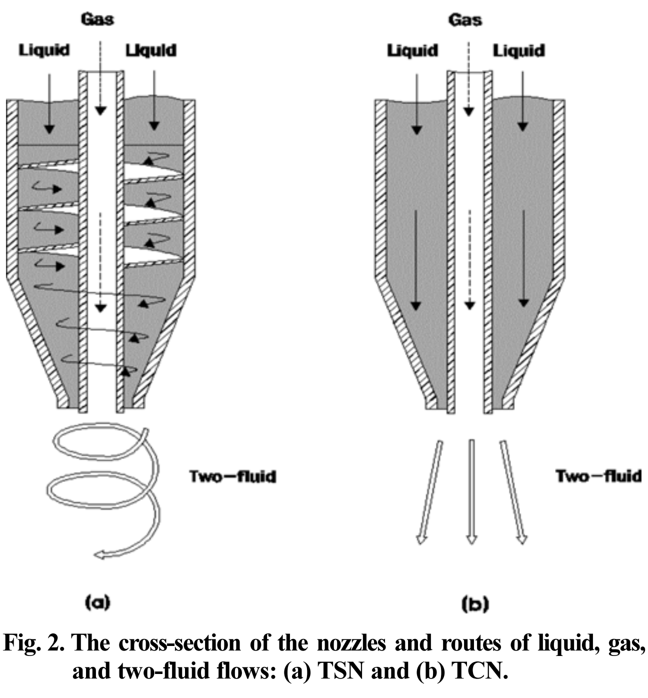

Fig. 2. The cross-section of the nozzles and routes of liquid, gas, and two-fluid flows: (a) TSN and (b) TCN.

A liquid storage tank with a height of 1.15 m, a diameter of 0.92 mm, and a total volume of 600 L was used. The liquid storage tank contained an alkaline solution with a pH of 10.1 and 60 ppm of NH_3-N, which was manufactured by injecting NaOH and NH_4Cl into tap water. A volumetric pump (WT600-2J, Longer Co., China) with rotation rate of 60-600 rpm, and cir- culation pump (PSS80-066, Hanil Co., South Korea) with a maximum discharge amount of 80 L/min, were used; and the CO_2 bomb was filled with gas mixture of 85% air and 15% CO_2.

To operate the equipment, the jet loop reactor was filled with 28.5 L of alkaline solution using the volumetric pump, and the alkaline solution flowed into the liquid induction tube with the two-fluid nozzle using the circulation pump. Simultaneously, the gas containing CO_2 was supplied through the gas induction tube. Circulation and gas dispersion were achieved by a liquid jet drive at the nozzle tip. At this moment, when the TCN was used (Fig. 2(a)), liquid and gas each were vertically discharged at the nozzle tip and formed a two-fluid (gas and liquid) liquor. The two-fluid liquor indicates the liquid stream in which small gas bubbles are homogeneously dispersed. The two-fluid liquor then passed down vertically the draft tube and up the outer annulus of the reactor [8,9,11]. When the TSN was used, at the nozzle tip, gas was vertically discharged; however, liquid was tangentially discharged by a swirl guide attached in the liquid induction tube. As mentioned earlier, the two-fluid liquor passed down tangentially the draft tube and up the outer annulus of the reactor. This swirling flow in the draft tube and the annular space was visually observed throughout this experiment. During this process, parts of the two-fluid liquor ascended along the streamline close to the outer wall of the draft tube and recirculated into the draft tube. However, the liquor that flowed close to the outer wall of the reaction tube (that is, the liquor that flowed far from the outer wall of the draft tube) from the upward stream did not recirculate and flowed into the gas-liquid separation tank. Among gas and liquid in the two-fluid liquor that flowed into the gas-liquid separation tank, the gas was separated and discharged through the gas discharge valve in the upper part, and the liquid in the gas-liquid separation tank was recirculated through the circulation pump to outside the reactor and discharged again through the two-fluid nozzle.

To compare the performance levels of the TCN and the TSN in the semi-batch mode, the reactors which the TCN and the TSN were separately attached were initially filled with 28.5 L of the alkaline solution. The circulation flow rates of the alkaline solution were changed to 12-32 L/min, and the pH variations of the alkaline solution were measured at a constant gas flow rate (1 L/min). The time it takes for the pH of the alkaline solution to be neutralized from 10.1 to 7.0 was defined as the neutralization time. In addition, the CO_2 mole fraction, among the discharged gases, was continuously measured at constant time intervals (2 minutes) from the CO_2 injection time using a CO_2 gas analyzer (Optima 7, MRU Instruments, Inc., Germany). Here, the instantaneous CO_2 removal efficiency and the overall CO_2 removal efficiency were calculated from the measurement results.

RESULTS AND DISCUSSION

1. Neutralization Time Dependence on Changes in the Liquid Circulation Flow Rate

To compare the performance of the TCN and the TSN in the semi-batch mode, the pH variation characteristics affected by the changes in the liquid circulation flow rates (Q_R=12-32 L/min) were measured.

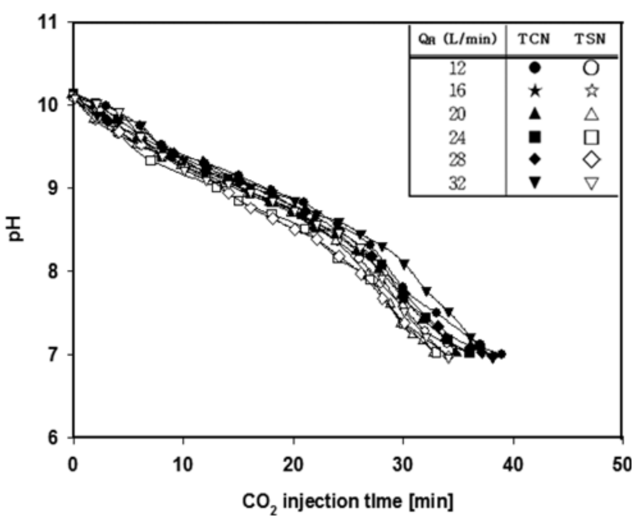

Fig. 3. pH changes with respect to the liquid circulation flow rates in the reactors with TCN and TSN.

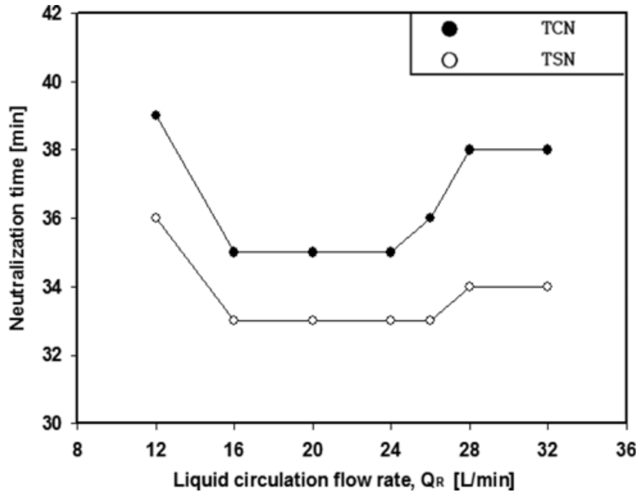

Fig. 4. Effect of the liquid circulation flow rate on the neutralization time.

This took place while the gas was continuously being injected into the jet loop reactors to which each nozzle was attached separately at a constant gas flow rate of 1 L/min (Fig. 3).

Fig. 3 shows the tendency of the alkaline solution to be neutralized and of the pH to decrease during the continuous injection of the gas with an inlet CO_2 mole fraction of 0.15. This is attributed to the absorption of the CO_2 in the gas into the alkaline solution, its reaction with OH^-, and its neutralization of the solution. Based on such results, the time required for the pH of the initial alkaline solution to change from 10.1 to 7.0 due to the changes in the liquid circulation flow rate (Q_R) in the cases with different types of nozzles, that is, the neutralization time, was measured. The results are shown in Fig. 4.

The two types of nozzles presented different neutralization times but showed equal neutralization time tendencies (Fig. 4). The neutralization time decreased with the increase in the liquid circulation flow rate (Q_R), reached its minimum value at 16-24 L/min, and increased with a further increase in the Q_R. These results showed trends similar to those of the results of the study of Son et al. [13], due to the increase in the turbulence intensity as the liquid circulation flow rate increased. Due to the increase in the mass transfer rate in the gas-liquid system, the neutralization time decreased. However, the neutralization time increased with a further increase in the liquid circulation flow rate. With the increase in the liquid circulation flow rate, the residence time of the gas bubbles in the gas-liquid system decreased despite the increase in turbulence intensity. The absolute values in the results of this study appear different from those of the study of Son et al. [13], presumably due to the difference in the quantity of the alkaline solution used.

In most cases, the neutralization time was shorter with the TSN than with the TCN at the same liquid circulation flow rate (Fig. 4). This result is attributed to the swirling flow formed at the nozzle tip of the TSN. By design, the TSN forms swirling flow and enhances the turbulence intensity in the gas and liquid films, therefore resulting in an improved mass transfer rate between the gas and the liquid, compared to the TCN [14,15].

2. CO_2 Removal Efficiency

2-1. Instantaneous CO_2 Removal Efficiency

The variations in the alkaline solution pH and the CO_2 mole frac-

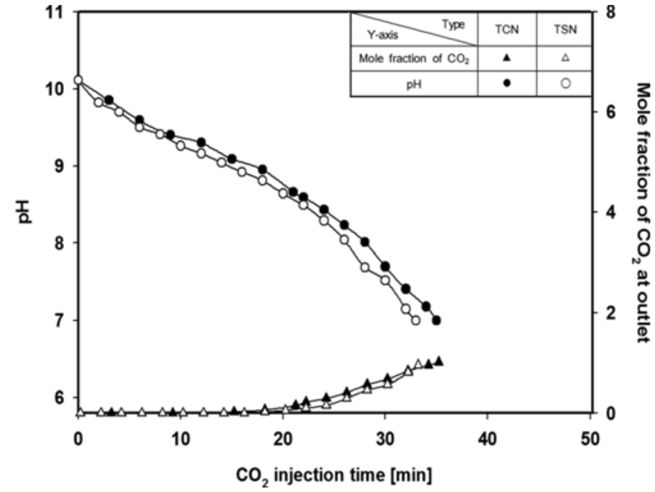

Fig. 5. Effects of the CO_2 injection time on alkaline solution pH and mole fraction of CO_2 at the outlet (Q_G=1 L/min, Q_R= 20 L/min).

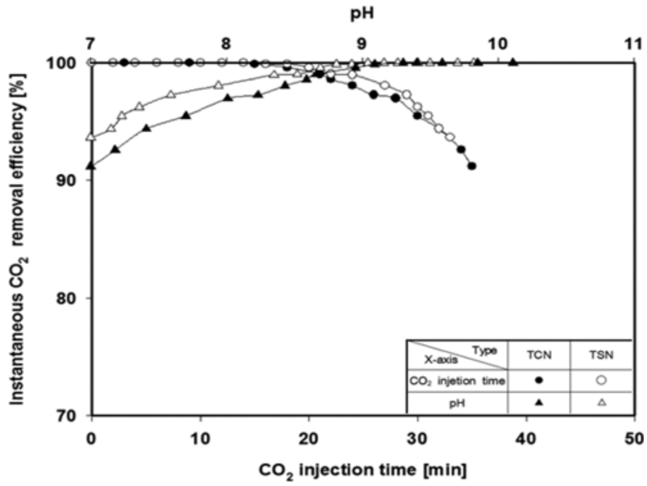

Fig. 6. Effect of the CO_2 injection time and the solution pH on the instantaneous CO_2 removal efficiency (Q_R=20 L/min).

tion in the outlet gas stream according to the CO_2 injection time were measured at constant time intervals (2 minutes) under the experimental conditions that were used, which are shown in Fig. 5.

Fig. 5 shows the tendencies of the pH of the alkaline solution to decrease and of the CO_2 mole fraction in the outlet gas to increase with the CO_2 injection time. Such results are attributed to the decrease in the solution pH with its neutralization by CO_2 absorption.

The CO_2 mole fraction in the outlet gas stream increased as the solution pH decreased by following reaction mechanism during the CO_2 absorption in the alkaline solution [16,17].

$$CO_2(g)+H_2O \Leftrightarrow CO_2(aq) \tag{1}$$

$$CO_2(aq)+OH^- \Leftrightarrow HCO_3^- \tag{2}$$

$$HCO_3^-+OH^- \Leftrightarrow CO_2^{2-}+H_2O \tag{3}$$

In the alkaline solution with higher pH, the CO_2 (aq) absorbed in the solution with reaction (1) was quickly consumed by reactions (2) and (3) because of the high OH^- concentration. However, reaction (2) was limited by the lower OH^- concentration in the solution with lower pH. Therefore, the CO_2 mole fraction in the outlet gas increased with the lower alkaline solution pH.

The instantaneous CO_2 removal efficiency at the arbitrary time t, can be calculated using Eq. (4), with the measurement results (Fig. 5) for the CO_2 mole fraction in the inlet gas injected into the reactor and in the outlet gas discharged from the reactor [13].

$$\eta_{CO_2}(\%)=\frac{Q_{G,in}\times y_{CO_2,in}-Q_{G,out}\times y_{CO_2,out}}{Q_{G,in}\times y_{CO,in}}\times 100 \tag{4}$$

In Eq. (4), η_{CO_2} represents the instantaneous CO_2 removal efficiency; Q_G, the inlet gas flow rate; y_{CO_2}, the CO_2 mole fraction; and the subscripts 'in' and 'out' represent the inlet and outlet of the reactor, respectively.

$Q_{G,out}$ can also be expressed as follows.

$$Q_{G,out}=Q_{G,in}\times\frac{y_{air,in}}{y_{air,out}} \tag{5}$$

Accordingly, the instantaneous CO_2 removal efficiency can be written as follows by substituting Eq. (5) into Eq. (4).

$$\eta_{CO_2}(t)(\%)=\frac{Q_{G,in}\times y_{CO_2,in}-Q_{G,in}\times y_{CO_2,out}\times\frac{y_{air,in}}{y_{air,out}}}{Q_{G,in}\times y_{CO,in}}\times 100 \tag{6}$$

Therefore, the CO_2 mole fractions in the inlet and outlet of the reactor at constant time intervals (2 minutes) from the initial CO_2 injection were measured and used to calculate the instantaneous CO_2 removal efficiency (Fig. 6).

As shown in Fig. 6, the instantaneous CO_2 removal efficiency decreased as the CO_2 injection time, i.e., the CO_2 injection amount, increased. This result is attributed to the decrease in solution pH as the alkaline solution was neutralized with increased CO_2 injection.

In addition, the instantaneous CO_2 removal efficiency appeared higher when the TSN was used with the same CO_2 injection time. This is attributed to the shrinkage of the bubbles, the increase in the turbulence intensity, and the longer retention time of small bubbles due to the swirling flow formed by the TSN. These effects resulted in improved mass transfer rate between the gas and liquid films.

The results shown in Fig. 5 were used to represent the instantaneous CO_2 removal efficiency depending on the changes in the pH of the alkaline solution (Fig. 6).

As shown in Fig. 6, the instantaneous CO_2 removal efficiency appeared higher in the alkaline solution at a higher pH and decreased as the solution pH decreased. According to previous studies [16, 17], reaction (2) is the rate-determining step among the CO_2 absorption reactions in an alkaline solution. Furthermore, reaction (2) represents an irreversible reaction, and its reaction rate appears as a second-order reaction, as follows [16,17]:

$$r_{HCO_3^-}=k_2[CO_2][OH^-] \tag{7}$$

Therefore, the reaction rate of reaction (2) increased when the alkaline solution pH remained high and the instantaneous CO_2 removal efficiency appeared higher.

In addition, the instantaneous CO_2 removal efficiency tended to decrease in both the TCN and the TSN as the solution pH decreased. However, the case with the TSN presented a higher instantaneous CO_2 removal efficiency than the case with the TCN under the same

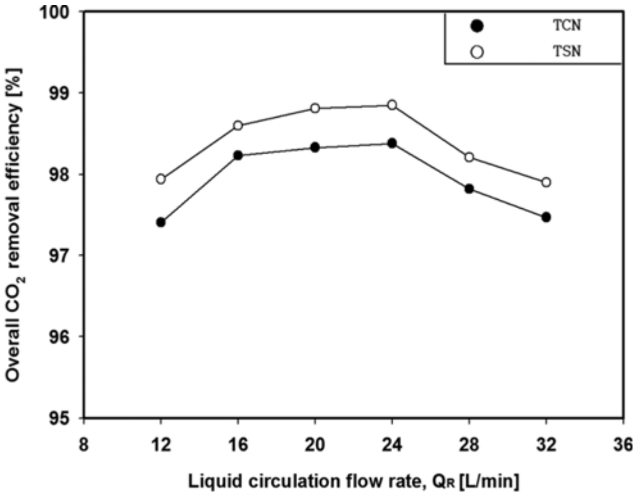

Fig. 7. Effect of the liquid circulation flow rate on the overall CO_2 removal efficiency.

solution pH, due to higher turbulence intensity and the longer retention time of bubbles formed by the TSN.

2-2. Overall CO_2 Removal Efficiency

The overall CO_2 removal efficiency ($\overline{\eta_{CO_2}}$), which was calculated using the time-integral value of the instantaneous CO_2 removal efficiency derived from Eq. (6), is defined as the CO_2 actually used to neutralize the initial alkaline solution pH from 10.1 to 7.0. The relationship between the instantaneous CO_2 removal efficiency and the overall CO_2 removal efficiency is as follows (Eq. (8)):

$$\overline{\eta_{CO_2}}(\%) = \frac{\sum(\eta_{CO_2}(\mathrm{t}) \times \Delta \mathrm{t})}{\mathrm{t}_{pH=7} - \mathrm{t}_0} \tag{8}$$

Here, $\eta_{CO_2}(t)$ refers to the instantaneous CO_2 removal efficiency; Δt, to the constant time interval (2 minutes); $t_{pH=7}$, to the neutralization time; and t_0, to the initial time (zero).

As shown in Fig. 7, there is an optimum range where the overall CO_2 removal efficiency peaks as the liquid circulation flow rate increases. The peaking of overall CO_2 removal efficiency was expected from the previous results (Fig. 4) and showed maximum value when the liquid circulation flow rate ranged from 16 to 24 L/min.

Both nozzles presented that the overall CO_2 removal efficiency was higher than 97%, likely due to the enlargement of the jet loop reactor in the interfacial area between gas and liquid films. The enlargement was attributed to the creation of minute bubbles, and to the achievement of a high mass transfer rate due to the significant turbulence intensity and the longer retention time of small bubbles. In addition, a higher overall CO_2 removal efficiency was shown at the same liquid circulation flow rates when the TSN was used.

CONCLUSIONS

To investigate the performance of a jet loop reactor with the two-fluid swirl nozzle (TSN), CO_2 absorption experiments in the reactor were performed in an alkaline solution. The results obtained were compared with the same sized jet loop reactor with the two-fluid conventional nozzle (TCN). The following conclusions were made.

1. At constant gas flow rate (Q_G=1 L/min), the neutralization times in the jet loop reactors with both the TCN and the TSN decreased with the liquid circulation flow rate (Q_R), reached their minimum value in the Q_R range of 16-24 L/min, and increased with a further increase in the Q_R. Furthermore, the neutralization time decreased in the case of the TSN compared to that of the TCN at the same Q_R.

2. When CO_2 gas was continuously injected into the jet loop reactors with both the TCN and the TSN, at an arbitrary time t, the instantaneous CO_2 removal efficiency appeared higher when the TSN was used. Moreover, the instantaneous CO_2 removal efficiency showed an increasing tendency as the alkaline solution pH increased.

3. The overall CO_2 removal efficiency peaked in the Q_R range of 16-24 L/min in both cases when TCN and TSN were used. However, the overall CO_2 removal efficiency was higher when the TSN was used at the same liquid circulation flow rate.

ACKNOWLEDGEMENTS

This study was supported by the New & Renewable Energy Project of the Korea Institute of Energy Technology Evaluation and Planning (KETEP) through a grant from the Ministry of Knowledge Economy (No. 2011T100200204).

REFERENCES

1. Z. W. Cao, Z. X. Li and H. X. Yuan, *Environ. Eng.*, **1**, 102 (2007).
2. P. C. Luo, Z. Jiao, Z. X. Wang and Z. B. Zhang, *Chem. Ind. Times*, **18**, 35 (2004).
3. Z. Q. Niu, Y. C. Guo and W. Y. Lin, *Science in China Series E: Technol. Sci.*, **53**, 117 (2010).
4. D. Darmana, R. L. B. Henket, N. G. Deen and J. A. M. Kuipers, *Chem. Eng. Sci.*, **62**, 2556 (2007).
5. C. Fleischer, S. Becker and G. Eigenberger, *Chem. Eng. Sci.*, **51**, 1715 (1996).
6. S. W. Park, I. J. Sohn, D. W. Park and K. J. Oh, *J. Sep. Sci. Technol.*, **38**, 1361 (2003).
7. E. S. Gaddis, *Chem. Eng. Process.*, **38**, 503 (1999).
8. K. Bohner and H. Blenke, *Verfahrenstechnik*, **6**, 50 (1972).
9. R. Pohorecki and W. Moniuk, *Chem. Eng. Sci.*, **43**, 1677 (1998).
10. N. Degermenci, O. N. Ata and E. Yildiz, *J. Ind. Chem. Eng.*, **18**, 399 (2012).
11. S. H. Kang, K. S. Song and J. M. Lim, *J. Korean Solid Wastes Engineering Society*, **16**, 554 (1999).
12. P. Maurizio, E. Ana and F. Federico, *Process Biochem.*, **37**, 821 (2002).
13. M. K. Son, H. J. Sung and J. K. Lee, *J. Korean Society of Combustion*, **18**, 17 (2013).
14. J. K. Lee and M. K. Son, Korean Patent, KR-B-10-2012-0056631 (2012).
15. P. V. Danckwerts, *Ind. Eng. Chem.*, **43**, 1460 (1951).
16. Astarita and Giovanni, *Mass transfer with chemical reactions*, Amsterdam and London (1967).
17. P. V. Danckwerts, *Gas-liquid Reactions*, McGraw-Hill, New York (1970).
18. Y. Peng, B. Zhoa and L. Li, *Energy Procedia*, **14**, 1515 (2012).
19. Y. T. Shah, B. G. Kelkar, S. P. Godbole and W.-D. Deckwer, *AIChE J.*, **28**, 353 (1982).
20. F. Takemura and Y. Matsumoto, *Chem. Eng. Sci.*, **55**, 3907 (2000).